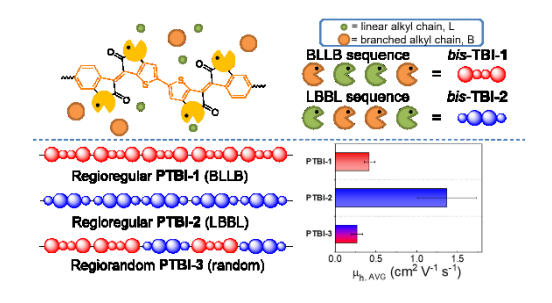
Side-chain Sequence Enabled Regioisomeric Acceptors for Conjugated Polymers

Xuyi Luo,[†] Dung T. Tran,[†] Natalie M. Kadlubowski,[†] Carr Hoi Yi Ho,[‡] Parand Riley,[‡] Franky So,[‡] and Jianguo Mei^{*†}

[†]Department of Chemistry, Purdue University, West Lafayette, Indiana 47907, United States

[‡]Department of Materials Science and Engineering, North Carolina State University, Raleigh, North Carolina 27606, United States



For Table of Contents Use Only

ABSTRACT: Side-chain sequence enabled regioisomeric acceptors, bearing different side-chain sequences on the same conjugated backbone, are herein reported. Two regioregular polymers PTBI-1, PTBI-2, and one regiorandom polymer PTBI-3 were synthesized from these two regioisomeric acceptors for a comparative study. UV-Vis-NIR absorption spectroscopy and electrochemical study confirmed similar frontier molecular orbital levels of the three polymers in

their solid state. More intriguingly, absorption profiles suggest that the sequence of side chains greatly governs the aggregation behaviors. Furthermore, the PTBI-2 film shows larger ordered domains than PTBI-1 and PTBI-3 films, as supported by AFM and GIWAXS measurements. As a result, PTBI-2-based FET devices achieved an average hole mobility of 1.37 cm²V⁻¹s⁻¹, much higher than the two polymers with other side-chain sequences. The regionandom PTBI-3 exhibited the lowest average hole mobility of 0.27 cm²V⁻¹s⁻¹. This study highlights the significant impact of side-chain sequence regioisomerism on aggregation behaviors, morphologies, and subsequently charge transport properties of donor-acceptor type conjugated polymers.

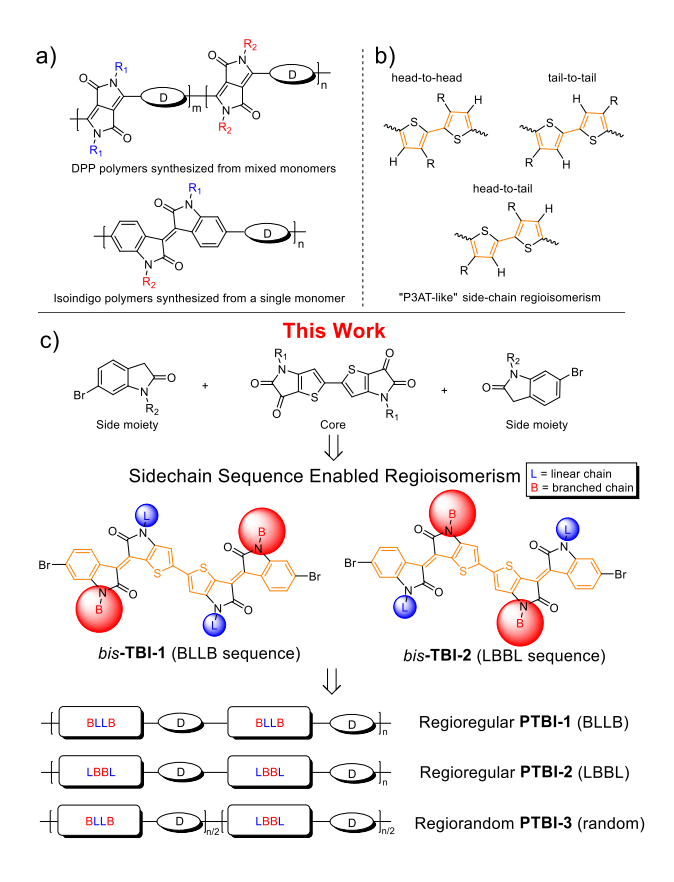
Introduction

Donor-acceptor (D-A) type conjugated polymers have attracted a great deal of attention as organic semiconductors in printed and flexible electronics because of the versatile chemistry available to tune their optical and electronic properties. $^{1-4}$ This potential has spurred the development of numerous π -conjugated polymer systems. $^{5-9}$ In molecular design of D-A polymers, side chain engineering has proved to be effective in tuning electronic and morphological properties of resulting polymer thin films. $^{10-16}$ Rational combination of different side chains is one of such strategies. $^{17-21}$ There are generally two approaches to introduce a combination of side chains. The first approach deals with the copolymerization of two monomers bearing the targeted side chains (Scheme 1a). For an example, Zhang *et. al.* developed a DPP (diketopyrrolopyrrole) monomer bearing urea-containing alkyl chains. 15 Changing the ratio of the urea-chain DPP monomers to the branched-alkyl-chain DPP monomers in polymerization provided a series of DPP random copolymers with enhanced charge mobilities. The second approach involves a single monomer bearing two different side chains, which would produce alternating copolymers (Scheme 1a). We

previously reported such an isoindigo building block with one alkyl chain and one siloxane hybrid chain.²² The corresponding polymer thin films adopted bimodal packing orientation and exhibited improved charge transport performance.

The presence of different types of side chains brings up the issue of side-chain sequence along the polymer backbones. It has been repeatedly shown in the case of polyalkylthiophenes that the side-chain sequence affects both physical and electronic properties.²³ (Scheme 1b) However, little has been known about side-chain regioisomerism in D-A polymers.^{24,25} Herein, we demonstrate for the first time side-chain sequence enabled regioisomeric acceptors for D-A copolymers based on the bis-thieno-benzo-isoindigo (bis-TBI) acceptor-acceptor type building block. (Scheme 1c) Owing to its convergent synthetic approach, two pairs of side chains can be efficiently mounted onto bis-TBI compound.²⁶ In the current study, bulky branched alkyl chains (B) and linear alkyl chains (L) are placed in two different sequences along the backbones, providing side-chain regioisomeric monomers bis-TBI-1 with a branched-linear-linear-branched (BLLB) side chain sequence and bis-TBI-2 with a linear-branched-branched-linear (LBBL) side chain sequence. It is worth noting that the two monomers share an identical conjugated core but with different side chain sequences away from the charge transport pathway, hence they are a different category of isomers than P3AT-like regioisomers. The corresponding D-A copolymers PTBI-1, PTBI-2, and a regiorandom copolymer PTBI-3 with mixed bis-TBI moieties are subsequently prepared to investigate the impact of side-chain-sequence regioisomerism on aggregation behaviors and charge transport properties of the polymers.

Scheme 1. Previous work, and illustration of the design rationale for *bis*-TBI regioisomeric acceptors



Results and discussion

Synthesis and characterization. The synthesis of PTBI polymers follows a similar convergent synthetic route we previously developed for *bis*-TBI moieties, ²⁶ as illustrated in Scheme 2. The core bis-thieno-isatin 3 bearing one type of side chain and the side moiety oxindole 5 bearing the other type were synthesized in good yields. After an aldol condensation reaction of compounds 3 and 5, regioisomers *bis*-TBI-1 (with BLLB sequence) and *bis*-TBI-2 (with LBBL sequence) were obtained in 76% and 86% yield respectively. Subsequently, Stille polymerization of *bis*-TBI monomers with bithiophene ditin compound 6 provided two regionegular PTBI polymers PTBI-1, PTBI-2 in 85% and 83% yields. The regionandom PTBI-3 were also synthesized from the 1:1 *bis*-TBIs mixture and compound 6, giving a 79% yield. Due to solubility issue, all polymerizations were carried out for 1 h. The synthesis detail is described in the Supporting Information. All polymers were purified by the Soxhlet extraction and fully characterized.

Molecular weights of PTBI polymers were evaluated by high-temperature gel permeation chromatography (Figure S1). All of PTBI polymers were estimated to have number-average molecular weights around 9 KDa and polydispersity indices (PDI) around 1.5. Similar molecular weight and polydispersity exclude the potential molecular weight effect when comparing PTBI polymers.²⁷

Scheme 2. The synthetic route to *bis*-TBI monomers and PTBI polymers

a) potassium phthalimide, DMF, 80 °C, overnight, 90%; b) Hydrazine hydrate, MeOH, reflux, 12 h, 95%; c) alkylamine, CuI, K₃PO₄, DMEA, 80 °C, 48 h; d) Oxalyl chloride, NEt₃, DCM, 0 °C to RT, overnight, 26% (**2a**) / 17% (**2b**) over two steps; e) AgF, Pd(OAc)₂, DMSO/dioxane, 90 °C, 24 h, 47% (**3a**) / 60% (**3b**); f) K₂CO₃, alkyl halide, DMF, 100 °C, overnight, 69% (**4a**) / 83% (**4b**); g) Hydrazine hydrate, DMSO, 130 °C, 24 h, 61% (**5a**) / 71% (**5b**); h) PTSA, Toluene, 110 °C, 12 h, 76% (*bis*-**TBI-1**) / 86% (*bis*-**TBI-2**); i) Pd₂(dba)₃, P(o-tol)₃, Toluene, 110 °C, 1 h, 79%-85%.

Electrochemical and Optical Properties. The redox properties of PTBI polymers were evaluated by cyclic voltammetry (CV) and differential pulse voltammetry (DPV). Cyclic voltammograms of all polymer thin films show similar redox profiles and quasi-reversible redox behavior (Figure 1). HOMO/LUMO energy levels of PTBI polymers were estimated from the respective redox onset potentials of both CV and DPV. As summarized in Table 1, all three polymers show similar HOMO/LUMO levels within a range of 0.03 eV. The side-chain sequence has little impact on electrochemical properties of PTBI polymers. It is worth noting that for polymers having alkyl chain substitution positions directly on aromatic rings (*i.e.* P3AT-like side-chain regioisomers), their regioisomers typically present a noticeable HOMO/LUMO energy level difference.^{24,25,28}

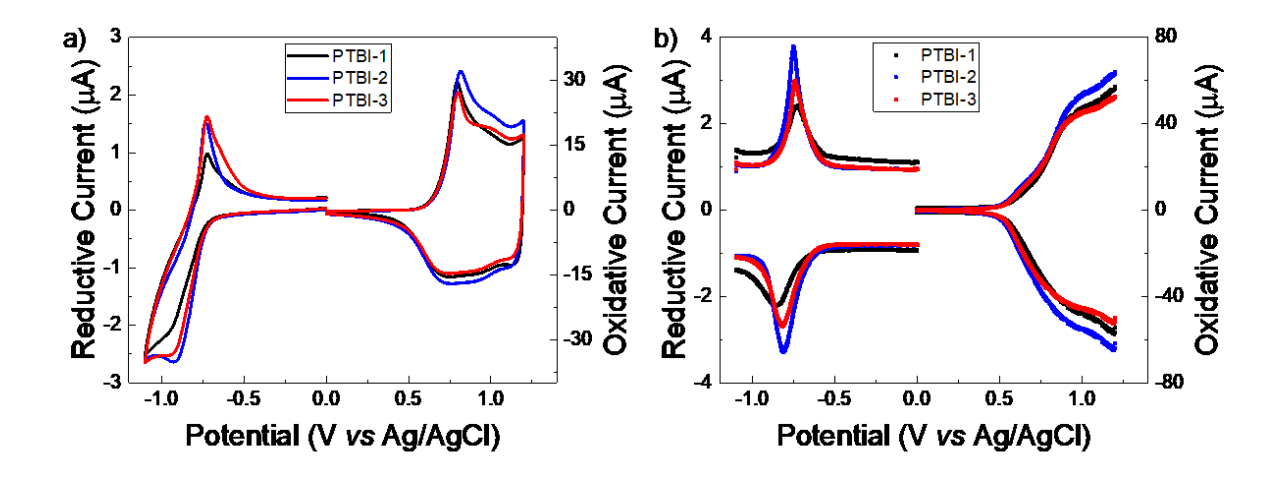


Figure 1. a) Cyclic Voltammograms of PTBI-1 (black), PTBI-2 (blue) and PTBI-3 (red); b) Differential pulse voltammograms of PTBI-1 (black), PTBI-2 (blue) and PTBI-3 (red). All polymer thin films were tested in propylene carbonate with 0.2 M *n*-Bu₄NPF₆ as supporting electrolyte (scan rate: 20 mV s⁻¹).

Photophysical properties of bis-TBI monomers and their polymers were characterized by solution and solid-state UV-Vis-NIR spectroscopy. As shown in figure 2a, two bis-TBI monomers bis-TBI-1 and bis-TBI-2 exhibit identical absorption profiles in diluted chloroform solutions, suggesting that their absorption properties are not influenced by the sequence of side chains in solutions. This observation is in a good agreement with their ¹H–NMR spectra collected in CDCl₃ solutions, where the two isomers have identical chemical shifts in the aromatic region. (Figure S2) Unexpectedly, the two isomers exhibit distinctly different absorption profiles in the solid states. bis-TBI-1 film presents a large blue shift of maximum absorbance (λ_{max}) from 726 nm to 652 nm from solution to thin film, while bis-TBI-2 film shows a strongly red-shifted absorption with λ_{max} at 815 nm in thin films. The blue and red shifts are attributed to two different packing motifs with predominant H- and J- aggregates respectively, ^{29,30} highlighting the crucial rule of the side-chain sequence in the highly aggregated bis-TBI molecules. Side-chain sequence also impacts photophysical properties of PTBI polymers, as shown by the solution and thin-film absorption profiles (Figure 2b and 2c). All polymers exhibit typical charge transfer peaks from 600 nm to 1100 nm. Peaks at around 950 nm and shoulders at around 870 nm are attributed to origin θ - θ and sideband 0-1 vibronic transitions respectively. Different from solutions of their monomers, the absorption spectra of PTBI polymers in dichlorobenzene (o-DCB) have a noticeable difference. Although PTBI polymers show nearly overlapped solution absorption profiles and λ_{max} , the relative intensities of 0-0 and 0-1 vibrational peaks of these polymers are different. It suggests that PTBI polymers form different pre-aggregates in solution. Thin-film absorption spectra of PTBI spun from ODCB solutions also have clear 0-0 and 0-1 vibrational peaks, indicative of their different solid-state packing. Identical film absorption onsets at 1047 nm suggest all polymers have

the same optical bandgap of 1.18 eV, consistent with the electrochemical estimations.

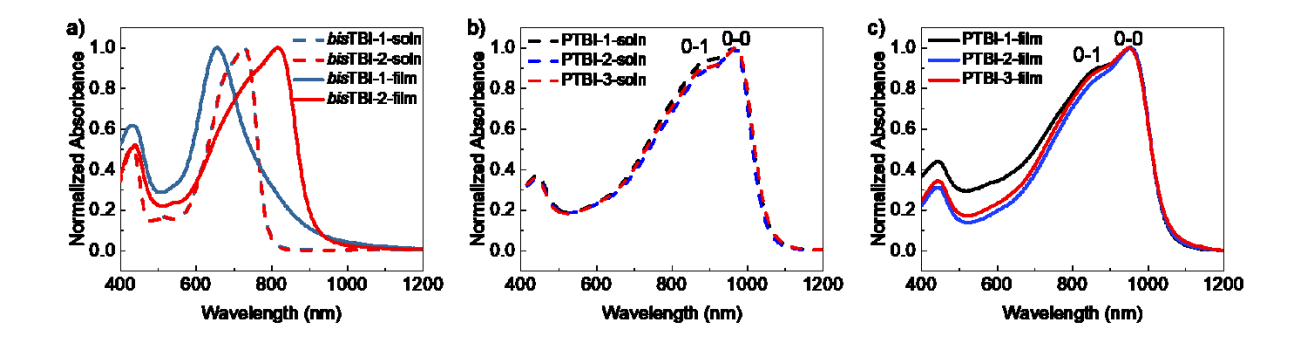


Figure 2. a) Solution and film Absorption spectra of *bis*-TBI-1 (blue) and *bis*-TBI-2 (red) in chloroform $(1.0 \times 10^{-5} \text{ M})$ (dashed line) and as film (solid line); b) Absorption spectra of PTBI-1 (black), PTBI-2 (blue), PTBI-3 (red) in *o*-DCB $(1.0 \times 10^{-5} \text{ M})$; c) Absorption spectra of PTBI-1 (black), PTBI-2 (blue), PTBI-3 (red) thin films spun from *o*-DCB solution.

Table 1. Optical and electrochemical properties of PTBI polymers

Polymer	Film absorption spectroscopy		Cyclic Voltammetry ^[b]			Differential Pulse Voltammetry ^[b]		
	Onset (nm)	$\begin{array}{c} E_g \\ (eV)^{[a]} \end{array}$	LUMO (eV)	HOMO (eV)	E _g (eV)	LUMO (eV)	HOMO (eV)	E _g (eV)
PTBI-1	1047	1.18	4.01	5.42	1.41	4.06	5.28	1.22
PTBI-2	1047	1.18	4.01	5.43	1.42	4.07	5.25	1.18
PTBI-3	1048	1.18	4.01	5.42	1.41	4.08	5.26	1.18

[[]a] Optical band gaps are estimated from E_g = 1240 nm/ λ_{onset} ; [b] The HOMO and LUMO energy levels are estimated from HOMO = - (5.10 + E_{ox} – $E_{Fc/Fc+}$) and LUMO = - (5.10 + E_{red} – $E_{Fc/Fc+}$), where E_{ox} and E_{red} are onset potentials.

Film morphology and microstructural analysis. Polymer thin film morphologies were analyzed by tapping-mode atomic force microscopy (AFM). All PTBI polymer films were spin coated from *o*-DCB solution on OTS-modified Si/SiO₂ substrates. As depicted in Figure 3, surface topography images of the PTBI-2 film show a smooth surface with crystalline fibrillar intercalating

networks, while PTBI-1 and PTBI-3 films show less ordered structures and mesh-like morphologies. PTBI-1 and PTBI-2 have similar root-mean-square (RMS) roughness of 0.69 and 0.64 nm respectively, while PTBI-3 has a slightly rougher surface with RMS roughness of 1.1 nm. Varying the annealing temperature didn't change film morphology features (Figure S5). The comparison of PTBI polymer films provides clear evidence that the microstructure is affected by side-chain sequence regioisomerism.

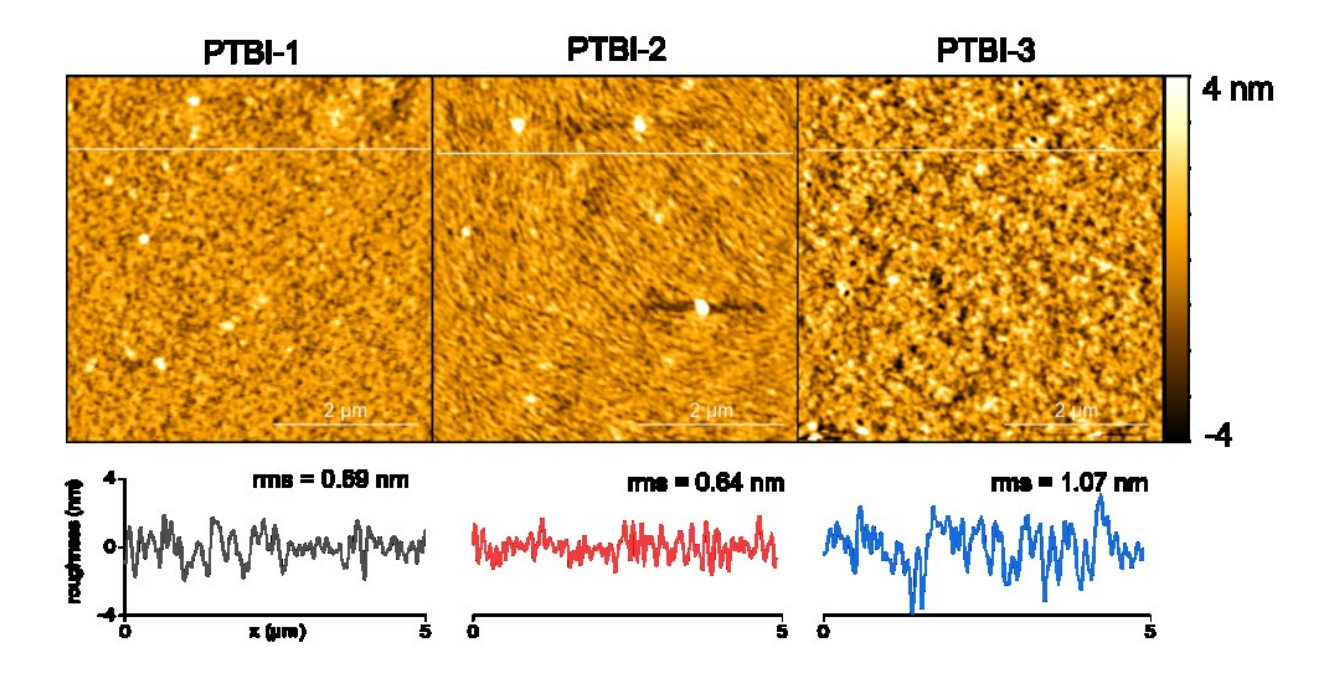


Figure 3. AFM height images of PTBI polymer thin films and the corresponding film roughness along white line profiles in the graphs for each film.

Grazing Incident X-ray Diffraction (GIXRD) measurements of thermally annealed PTBI polymer films were also carried out to obtain further insights into molecular packing in thin films. All three polymers show bimodal packing with both edge-on ($\chi=90^{\circ}$) and face-on ($\chi=0^{\circ}$) orientations of π - π stacking. Such bimodal orientation is considered to be beneficial for charge transport in the previous reports (Figure S6). 10,22,31 Long range ordered lamellar packings up to

(400) peak along face-on direction were also observed for all three polymers. As summarized in Table 2, the observed shortest π - π stacking distance among the three polymers is 3.51 Å of PTBI-2, only slightly shorter than PTBI-1 (3.52 Å) and PTBI-3 (3.53 Å). The small difference of GIXRD patterns is distinctly different from P3AT-like regioisomerism. ^{24,25,28} PTBI-2 in-plane π - π stacking was estimated to have a significantly lower full-width half-maximum (FWHM) of 0.098 than PTBI-1 of 0.129 and PTBI-3 of 0.140, as shown in Figure 4. The same trend was also observed for out-of-plane (200) lamellar packing peaks. Although the three polymer films were estimated to have similar lamellar packing distances, PTBI-2 has a much smaller lamellar packing FWHM than other two polymers. According to Scherrer's equation, FWHM is inversely proportional to the crystal coherence length. ³² Thus, a lower FWHM value usually implies larger crystalline domains. These observations are in a good agreement with AFM images, where PTBI-2 film appears to have a morphology with larger ordered domains.

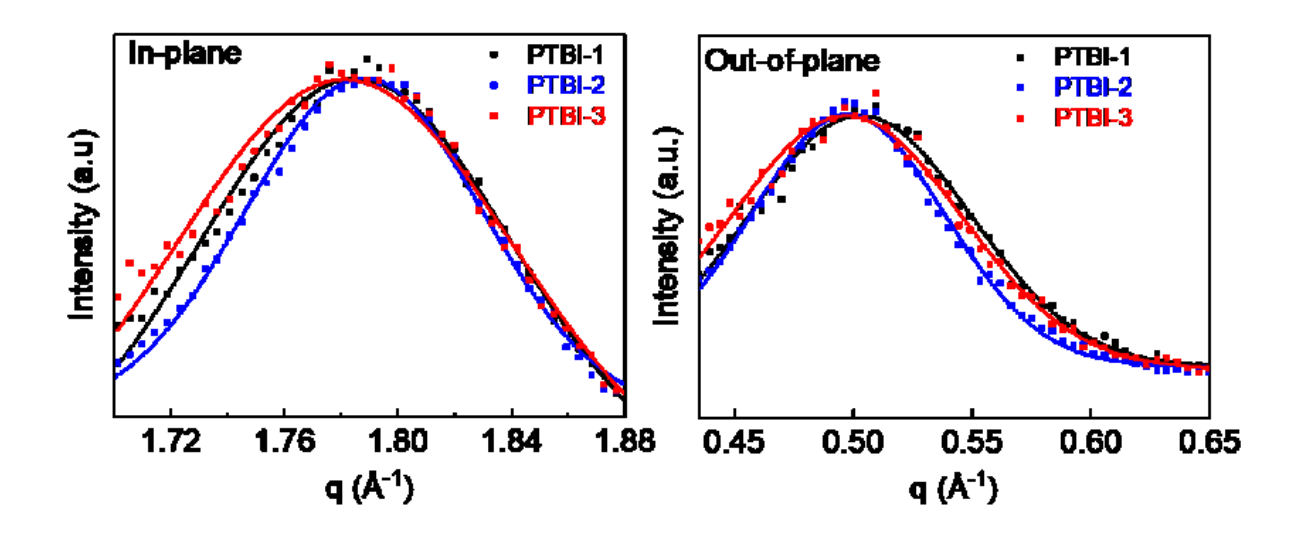


Figure 4. In-plane (010) and out-of-plane (200) plots of PTBI-1 (black), PTBI-2 (blue), PTBI-3 (red) and their fitted curves.

Table 2. Summary of 2D-GIXRD data and FET device performance of PTBI polymers

Polymer	π-π distance (Å)	FWHM in-plane (010)	lamellar distance (Å)	FWHM out-of- plane (200)	$\begin{array}{c} \mu_{ave} \\ (cm^2V^{-1} \\ s^{-1}) \end{array}$	μ _{max} (cm ² V ⁻¹ s ⁻¹)	Ion/off	V _{th} (V)
PTBI-1	3.52	0.129	24.6	0.109	0.40 ± 0.065	0.53	104	-8 ± 4
PTBI-2	3.51	0.098	24.6	0.095	1.37 ± 0.36	2.22	104	-5 ± 3
PTBI-3	3.53	0.140	24.8	0.114	0.27 ± 0.070	0.43	104	-8 ± 3

Charge transport measurements. To what extent side-chain sequence would impact charge transport properties is our primary interest of this study. Therefore, both field effect transistor measurements and space-charge-limited current (SCLC) method were employed to characterize charge mobilities of PTBI polymers. Details of the device fabrication are described in the Supporting Information. FET Devices of all PTBI polymer thin films with bottom-gate bottom-contact (BGBC) architecture and Au contacts under ambient conditions displayed p- type characteristics. (Figure 5) Charge mobilities of all polymers were calculated based on more than 15 devices. The average mobilities of PTBI-2, PTBI-3 and PTBI-3 were estimated to be 0.40, 1.37 and 0.27 cm²V⁻¹s⁻¹ respectively, and their corresponding highest mobilities were 0.53, 2.22 and 0.43 cm²V⁻¹s⁻¹. The current on/off ratios for all FETs are around 10⁴. The SCLC mobilities measured from hole-only diodes showed consistent trend with FET mobilities, where the mobilities of PTBI-2 (2.04 × 10⁻² cm²V⁻¹s⁻¹) were highest, PTBI-1 (1.85 × 10⁻² cm²V⁻¹s⁻¹) being the second highest and PTBI-3 (4.67 × 10⁻³ cm²V⁻¹s⁻¹) being the lowest. (Figure S7)

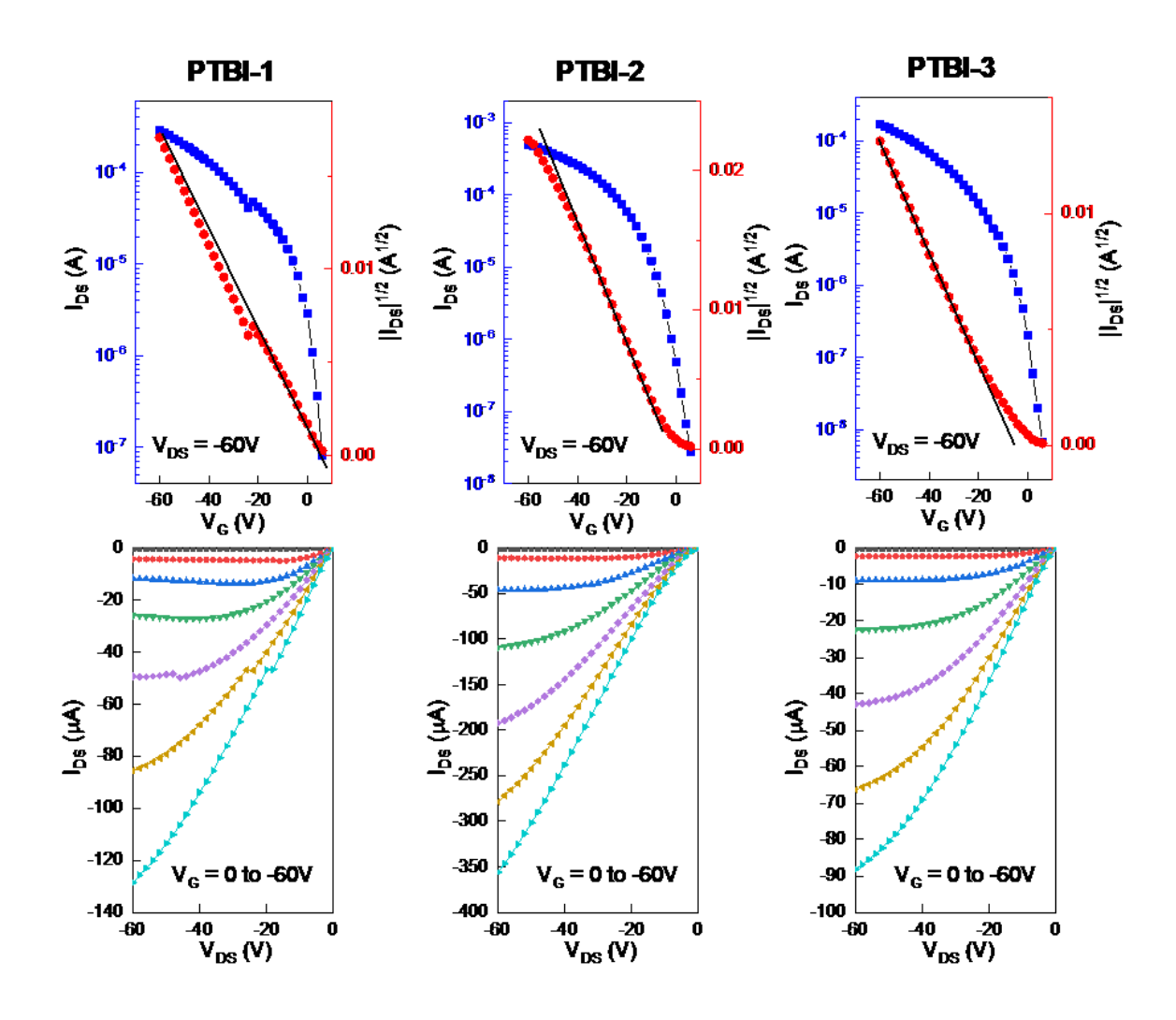


Figure 5. Representative transfer and output curves of PTBI-1, PTBI-2 and PTBI-3 thin film transistor devices.

The highest performance of PTBI-2 can be attributed to its fibrillar morphology and largest crystalline domain, as observed from AFM and 2D-GIXRD measurements. Similarly, poor performance of PTBI-3 film may result from the smallest crystalline domain, reconfirming negative effects of regionandom structures on polymer optoelectronic properties. ^{23,33,34} Intriguingly, although PTBI-1 is also a regionegular polymer like PTBI-2, noticeable differences were observed in solid state aggregation, morphology, crystalline domain size, and consequently device

performance of the two polymers. A possible reason for such differences is the steric effect of side chains between repeating units, as supported by many reports. ^{21,35–38} Density functional theory calculations predicted a good planarity within the *bis*-TBI accepting moiety and twisted conformation between the donors and acceptors. ²⁶ It is likely that the steric repulsion of side chains between *bis*-TBI and bithiophene (rather than inside the *bis*-TBI moiety) has a larger impact on the polymer chains. If the steric repulsion of side chains plays a role, the example of PTBI1- and PTBI-2 pairs provides a scenario implying that moving bulky solubilizing side chains inside the planar or rigid moiety could help improve charge transport properties. Considering most long rigid/fused conjugated building blocks have bulkier branched side chains at sides of moieties, ^{39–43} this side-chain regioisomerism strategy may serve as versatile tool to optimize the structure for enhanced charge transport purposes.

Conclusion

In summary, side-chain sequence enabled regioreisomeric acceptors for D-A type copolymers are first demonstrated. Starting with these *bis*-TBI monomers, three polymers PTBI-1, PTBI-2 and PTBI-3 were synthesized and fully characterized. The three polymers are similar in their frontier orbital energy levels but have distinct aggregation states in thin films. AFM and 2D-GIXRD measurements indicate that the PTBI-2 thin film shows smooth fibrillar morphology and the largest ordered domains. As a result, PTBI-2 FET devices achieved the highest hole mobility of 2.22 cm²V⁻¹s⁻¹, much higher than other two polymers with different side-chain sequences. We anticipate that the strategy of side-chain sequence regioisomerism could be applied in future design of building blocks for functional D-A type semiconducting polymers.

ASSOCIATED CONTENT

Supporting Information.

The Supporting Information is available free of charge.

Experimental details, figures and tables, and compound characterization data (PDF)

AUTHOR INFORMATION

Corresponding Author

*igmei@purdue.edu (J.M.).

Notes

The authors declare no competing financial interest.

ACKNOWLEDGMENT

The authors acknowledge the financial support from Purdue University and from the National Science Foundation (NSF CAREER Award, #1653909). Thanks to Ge Qu and Ying Diao for collecting the X-ray data. This research used resources of the Advanced Photon Source, a U.S. Department of Energy (DOE) Office of Science User Facility operated for the DOE Office of Science by Argonne National Laboratory under Contract No. DE-AC02-06CH11357.

REFERENCES

- (1) Forrest, S. R. The Path to Ubiquitous and Low-Cost Organic Electronic Appliances on Plastic. *Nature* **2004**, *428* (6986), 911–918.
- (2) Hammock, M. L.; Chortos, A.; Tee, B. C.-K.; Tok, J. B.-H.; Bao, Z. 25th Anniversary Article: The Evolution of Electronic Skin (E-Skin): A Brief History, Design Considerations, and Recent Progress. *Adv. Mater.* **2013**, *25* (42), 5997–6038.

- (3) Sirringhaus, H. 25th Anniversary Article: Organic Field-Effect Transistors: The Path Beyond Amorphous Silicon. *Adv. Mater.* **2014**, *26* (9), 1319–1335.
- (4) Fukuda, K.; Someya, T. Recent Progress in the Development of Printed Thin-Film Transistors and Circuits with High-Resolution Printing Technology. Adv. Mater. 2017, 29 (25), 1602736.
- (5) Würthner, F.; Stolte, M. Naphthalene and Perylene Diimides for Organic Transistors. *Chem. Commun.* **2011**, *47* (18), 5109.
- (6) Wang, E.; Mammo, W.; Andersson, M. R. 25th Anniversary Article: Isoindigo-Based Polymers and Small Molecules for Bulk Heterojunction Solar Cells and Field Effect Transistors. Adv. Mater. 2014, 26 (12), 1801–1826.
- (7) Guo, X.; Facchetti, A.; Marks, T. J. Imide- and Amide-Functionalized Polymer Semiconductors. *Chem. Rev.* **2014**, *114* (18), 8943–9021.
- (8) Yi, Z.; Wang, S.; Liu, Y. Design of High-Mobility Diketopyrrolopyrrole-Based π-Conjugated Copolymers for Organic Thin-Film Transistors. Adv. Mater. 2015, 27 (24), 3589–3606.
- (9) Quinn, J. T. E.; Zhu, J.; Li, X.; Wang, J.; Li, Y. Recent Progress in the Development of N-Type Organic Semiconductors for Organic Field Effect Transistors. *J. Mater. Chem. C* 2017, 5 (34), 8654–8681.
- (10) Mei, J.; Kim, D. H.; Ayzner, A. L.; Toney, M. F.; Bao, Z. Siloxane-Terminated Solubilizing Side Chains: Bringing Conjugated Polymer Backbones Closer and Boosting Hole Mobilities in Thin-Film Transistors. J. Am. Chem. Soc. 2011, 133 (50), 20130–20133.
- (11) Lei, T.; Dou, J.-H.; Pei, J. Influence of Alkyl Chain Branching Positions on the Hole Mobilities of Polymer Thin-Film Transistors. *Adv. Mater.* **2012**, *24* (48), 6457–6461.

- (12) Lee, J.; Han, A.-R.; Kim, J.; Kim, Y.; Oh, J. H.; Yang, C. Solution-Processable Ambipolar Diketopyrrole–Selenophene Polymer with Unprecedentedly High Hole and Electron Mobilities. *J. Am. Chem. Soc.* **2012**, *134* (51), 20713–20721.
- (13) Dou, J.-H.; Zheng, Y.-Q.; Lei, T.; Zhang, S.-D.; Wang, Z.; Zhang, W.-B.; Wang, J.-Y.; Pei, J. Systematic Investigation of Side-Chain Branching Position Effect on Electron Carrier Mobility in Conjugated Polymers. Adv. Funct. Mater. 2014, 24 (40), 6270–6278.
- (14) Kang, B.; Kim, R.; Lee, S. B.; Kwon, S.-K.; Kim, Y.-H.; Cho, K. Side-Chain-Induced Rigid Backbone Organization of Polymer Semiconductors through Semifluoroalkyl Side Chains. *J. Am. Chem. Soc.* 2016, 138 (11), 3679–3686.
- (15) Yao, J.; Yu, C.; Liu, Z.; Luo, H.; Yang, Y.; Zhang, G.; Zhang, D. Significant Improvement of Semiconducting Performance of the Diketopyrrolopyrrole—Quaterthiophene Conjugated Polymer through Side-Chain Engineering via Hydrogen-Bonding. *J. Am. Chem. Soc.* **2016**, *138* (1), 173–185.
- (16) Ocheje, M. U.; Charron, B. P.; Cheng, Y.-H.; Chuang, C.-H.; Soldera, A.; Chiu, Y.-C.; Rondeau-Gagné, S. Amide-Containing Alkyl Chains in Conjugated Polymers: Effect on Self-Assembly and Electronic Properties. *Macromolecules* 2018, 51 (4), 1336–1344.
- (17) Giovannitti, A.; Maria, I. P.; Hanifi, D.; Donahue, M. J.; Bryant, D.; Barth, K. J.; Makdah, B. E.; Savva, A.; Moia, D.; Zetek, M.; Barnes, P. R. F.; Reid, O. G.; Inal, S.; Rumbles, G.; Malliaras, G. G.; Nelson, J.; Rivnay, J.; McCulloch, I. The Role of the Side Chain on the Performance of N-Type Conjugated Polymers in Aqueous Electrolytes. *Chem. Mater.* 2018, 30 (9), 2945–2953.
- (18) Wen, H.-F.; Wu, H.-C.; Aimi, J.; Hung, C.-C.; Chiang, Y.-C.; Kuo, C.-C.; Chen, W.-C. Soft Poly(butyl Acrylate) Side Chains toward Intrinsically Stretchable Polymeric

- Semiconductors for Field-Effect Transistor Applications. *Macromolecules* **2017**, *50* (13), 4982–4992.
- (19) Yang, S.-F.; Liu, Z.-T.; Cai, Z.-X.; Dyson, M. J.; Stingelin, N.; Chen, W.; Ju, H.-J.; Zhang, G.-X.; Zhang, D.-Q. Diketopyrrolopyrrole-Based Conjugated Polymer Entailing Triethylene Glycols as Side Chains with High Thin-Film Charge Mobility without Post-Treatments. Adv. Sci. 2017, 4 (8), 1700048.
- (20) Ma, J.; Liu, Z.; Wang, Z.; Yang, Y.; Zhang, G.; Zhang, X.; Zhang, D. Charge Mobility Enhancement for Diketopyrrolopyrrole-Based Conjugated Polymers by Partial Replacement of Branching Alkyl Chains with Linear Ones. *Mater. Chem. Front.* 2017, 1 (12), 2547–2553.
- (21) Wang, Z.; Liu, Z.; Ning, L.; Xiao, M.; Yi, Y.; Cai, Z.; Sadhanala, A.; Zhang, G.; Chen, W.; Sirringhaus, H.; Zhang, D. Charge Mobility Enhancement for Conjugated DPP-Selenophene Polymer by Simply Replacing One Bulky Branching Alkyl Chain with Linear One at Each DPP Unit. *Chem. Mater.* 2018, 30 (9), 3090–3100.
- (22) Xue, G.; Zhao, X.; Qu, G.; Xu, T.; Gumyusenge, A.; Zhang, Z.; Zhao, Y.; Diao, Y.; Li, H.; Mei, J. Symmetry Breaking in Side Chains Leading to Mixed Orientations and Improved Charge Transport in Isoindigo- Alt -Bithiophene Based Polymer Thin Films. ACS Appl. Mater. Interfaces 2017, 9 (30), 25426–25433.
- (23) Ying, L.; Huang, F.; Bazan, G. C. Regioregular Narrow-Bandgap-Conjugated Polymers for Plastic Electronics. *Nat. Commun.* **2017**, *8*, 14047.
- (24) Quinn, J. T. E.; Guo, C.; Haider, F.; Patel, H.; Khan, D. A.; Li, Y. Regioisomerism of an Alkyl-Substituted Bithiophene Comonomer in (3E,8E)-3,8-bis(2-Oxoindolin-3-

- Ylidene)naphtho-[1,2-b:5,6-B']difuran-2,7(3H,8H)-Dione (INDF)-Based D-A Polymers for Organic Thin Film Transistors. *J. Mater. Chem. C* **2017**, *5* (24), 5902–5909.
- (25) Wang, X.; Choi, H. H.; Zhang, G.; Ding, Y.; Lu, H.; Cho, K.; Qiu, L. Bis(2-Oxoindolin-3-Ylidene)-Benzodifuran-Dione and Bithiophene-Based Conjugated Polymers for High Performance Ambipolar Organic Thin-Film Transistors: The Impact of Substitution Positions on Bithiophene Units. J. Mater. Chem. C 2016, 4 (26), 6391–6400.
- (26) Luo, X.; Tran, D. T.; Sun, H.; Mi, T.; Kadlubowski, N. M.; Zhao, Y.; Zhao, K.; Mei, J. Bis-Isoindigos: New Electron-Deficient Building Blocks for Constructing Conjugated Polymers with Extended Electron Delocalization. *Asian J. Org. Chem.* 2018, DOI: 10.1002/ajoc.201800360.
- (27) Cho, H. J.; Kang, S.-J.; Lee, S. M.; Jeong, M.; Kim, G.; Noh, Y.-Y.; Yang, C. Influence of Simultaneous Tuning of Molecular Weights and Alkyl Substituents of Poly(thienoisoindigo- Alt -Naphthalene)s on Morphology and Change Transport Properties.

 *ACS Appl. Mater. Interfaces 2017, 9 (36), 30755–30763.
- (28) Wang, X.-Y.; Zhang, M.-W.; Zhuang, F.-D.; Wang, J.-Y.; Pei, J. Lactone-Fused Electron-Deficient Building Blocks for N-Type Polymer Field-Effect Transistors: Synthesis, Properties, and Impact of Alkyl Substitution Positions. *Polym. Chem.* 2016, 7 (12), 2264–2271.
- (29) Kasha, M. Energy Transfer Mechanisms and the Molecular Exciton Model for Molecular Aggregates. *Radiat. Res.* **1963**, *20* (1), 55.
- (30) Más-Montoya, M.; Janssen, R. A. J. The Effect of H- and J-Aggregation on the Photophysical and Photovoltaic Properties of Small Thiophene-Pyridine-DPP Molecules for Bulk-Heterojunction Solar Cells. *Adv. Funct. Mater.* **2017**, *27* (16), 1605779.

- (31) Park, S.; Lee, M. H.; Ahn, K. S.; Choi, H. H.; Shin, J.; Xu, J.; Mei, J.; Cho, K.; Bao, Z.; Lee, D. R.; Kang, M. S.; Kim, D. H. Combinatorial Study of Temperature-Dependent Nanostructure and Electrical Conduction of Polymer Semiconductors: Even Bimodal Orientation Can Enhance 3D Charge Transport. Adv. Funct. Mater. 2016, 26 (26), 4627–4634.
- (32) Rivnay, J.; Mannsfeld, S. C. B.; Miller, C. E.; Salleo, A.; Toney, M. F. Quantitative Determination of Organic Semiconductor Microstructure from the Molecular to Device Scale. *Chem. Rev.* **2012**, *112* (10), 5488–5519.
- Ying, L.; Hsu, B. B. Y.; Zhan, H.; Welch, G. C.; Zalar, P.; Perez, L. A.; Kramer, E. J.; Nguyen, T.-Q.; Heeger, A. J.; Wong, W.-Y.; Bazan, G. C. Regioregular Pyridal[2,1,3]thiadiazole π-Conjugated Copolymers. J. Am. Chem. Soc. 2011, 133 (46), 18538–18541.
- (34) Wang, M.; Wang, H.; Yokoyama, T.; Liu, X.; Huang, Y.; Zhang, Y.; Nguyen, T.-Q.; Aramaki, S.; Bazan, G. C. High Open Circuit Voltage in Regioregular Narrow Band Gap Polymer Solar Cells. *J. Am. Chem. Soc.* **2014**, *136* (36), 12576–12579.
- (35) Durban, M. M.; Kazarinoff, P. D.; Luscombe, C. K. Synthesis and Characterization of Thiophene-Containing Naphthalene Diimide N-Type Copolymers for OFET Applications.

 *Macromolecules** 2010, 43 (15), 6348–6352.
- (36) Yi, Z.; Sun, X.; Zhao, Y.; Guo, Y.; Chen, X.; Qin, J.; Yu, G.; Liu, Y. Diketopyrrolopyrrole-Based π-Conjugated Copolymer Containing β-Unsubstituted Quintetthiophene Unit: A Promising Material Exhibiting High Hole-Mobility for Organic Thin-Film Transistors. *Chem. Mater.* 2012, 24 (22), 4350–4356.

- (37) Chen, M. S.; Lee, O. P.; Niskala, J. R.; Yiu, A. T.; Tassone, C. J.; Schmidt, K.; Beaujuge, P. M.; Onishi, S. S.; Toney, M. F.; Zettl, A.; Fréchet, J. M. J. Enhanced Solid-State Order and Field-Effect Hole Mobility through Control of Nanoscale Polymer Aggregation. *J. Am. Chem. Soc.* 2013, 135 (51), 19229–19236.
- (38) Grand, C.; Zajaczkowski, W.; Deb, N.; Lo, C. K.; Hernandez, J. L.; Bucknall, D. G.; Müllen, K.; Pisula, W.; Reynolds, J. R. Morphology Control in Films of Isoindigo Polymers by Side-Chain and Molecular Weight Effects. ACS Appl. Mater. Interfaces 2017, 9 (15), 13357–13368.
- (39) Lei, T.; Dou, J.-H.; Cao, X.-Y.; Wang, J.-Y.; Pei, J. Electron-Deficient Poly(P -Phenylene Vinylene) Provides Electron Mobility over 1 Cm 2 V -1 S -1 under Ambient Conditions. *J. Am. Chem. Soc.* **2013**, *135* (33), 12168–12171.
- (40) Cao, Y.; Yuan, J.-S.; Zhou, X.; Wang, X.-Y.; Zhuang, F.-D.; Wang, J.-Y.; Pei, J. N-Fused BDOPV: A Tetralactam Derivative as a Building Block for Polymer Field-Effect Transistors. *Chem. Commun.* **2015**, *51* (52), 10514–10516.
- (41) Dai, Y.-Z.; Ai, N.; Lu, Y.; Zheng, Y.-Q.; Dou, J.-H.; Shi, K.; Lei, T.; Wang, J.-Y.; Pei, J. Embedding Electron-Deficient Nitrogen Atoms in Polymer Backbone towards High Performance N-Type Polymer Field-Effect Transistors. *Chem. Sci.* **2016**, *7* (9), 5753–5757.
- (42) James, D. I.; Wang, S.; Ma, W.; Hedström, S.; Meng, X.; Persson, P.; Fabiano, S.; Crispin, X.; Andersson, M. R.; Berggren, M.; Wang, E. High-Performance Hole Transport and Quasi-Balanced Ambipolar OFETs Based on D-A-A Thieno-Benzo-Isoindigo Polymers. Adv. Electron. Mater. 2016, 2 (4), 1500313.

(43) Randell, N. M.; Radford, C. L.; Yang, J.; Quinn, J.; Hou, D.; Li, Y.; Kelly, T. L. Effect of Acceptor Unit Length and Planarity on the Optoelectronic Properties of Isoindigo—Thiophene Donor–Acceptor Polymers. *Chem. Mater.* **2018**, *30* (14), 4864–4873.